

# The Effect of the Architecture and Concentration of Styrene–Butadiene Compatibilizers on the Morphology of Polystyrene/Low-Density Polyethylene Blends

Ivan Fortelný,<sup>1,2</sup> Miroslav Šlouf,<sup>1</sup> Antonín Sikora,<sup>1,2</sup> Drahomíra Hlavatá,<sup>1</sup> Věra Hašová,<sup>1</sup> Jana Mikešová,<sup>1</sup> Ceni Jacob<sup>1</sup>

<sup>1</sup>Institute of Macromolecular Chemistry, Academy of Sciences of the Czech Republic, 162 06 Prague 6, Czech Republic

<sup>2</sup>Joint Laboratory for Polymer Materials of the Tomas Bata University Zlín and the Institute of Macromolecular Chemistry of the Academy of Sciences of the Czech Republic, 162 06 Prague 6, Czech Republic.

Received 31 January 2005; accepted 15 August 2005

DOI 10.1002/app.23731

Published online 9 February 2006 in Wiley InterScience (www.interscience.wiley.com).

**ABSTRACT:** The effect of styrene–butadiene block copolymers (SB) with varying number of blocks and length of styrene blocks on the morphology, rheology, and impact strength of 4/1 polystyrene/low-density polyethylene (PS/LDPE) blends was studied. The scanning and transmission electron microscopy and X-ray scattering were used for determination of the size of LDPE particles and the localization and structure of SB copolymers in blends. It is shown that the dependence of the LDPE particle size on the amount of added SB and localization of SB copolymers in blends is predominantly controlled by the length of their styrene blocks. It follows from thermodynamic considerations that the reason is the difference in composition asymmetry between SB with short and long styrene blocks. Coalescence of particles of SB having short styrene blocks at the surface of LDPE droplets and movement of SB with long styrene blocks to the PS–LDPE interface were observed during annealing of PS/LDPE/SB blends. Pronounced migration of SB copolymer during annealing shows that their localiza-

tions in blends in steady state on long steady mixing and at thermodynamic equilibrium are different. The values of tensile impact strength of PS/LDPE/SB blends correlate well with the size of LDPE particles and the amount of SB at the interface. Viscosity of PS/LDPE/SB depends on molecular structure of SB copolymers by a manner different from that of tensile impact strength. The results of this study and literature data lead to the conclusion that the compatibilization efficiency of SB copolymers for a certain polystyrene–polyolefin pair is a function of not only molecular parameters of SB but also of the polystyrene/polyolefin ratio, the amount of SB in a blend, and mixing and processing conditions. © 2006 Wiley Periodicals, Inc. *J Appl Polym Sci* 100: 2803–2816, 2006

**Key words:** polymer blends; compatibilization; styrene–butadiene block copolymers; polystyrene; low-density polyethylene

## INTRODUCTION

It is well known that block copolymers with blocks identical, miscible or adhering to the related components of a blend are suitable compatibilizers for immiscible polymer blends.<sup>1–4</sup> It was shown that the efficiency of block copolymers, i.e., the magnitude of their effect on the structure and properties of polymer blends, depends on their molecular parameters, such as the length and the number of blocks and interaction parameters,  $\chi$ , between the blocks and the related blend components. Discrepancies exist among simple

rules for prediction of the effect of the block copolymers architecture on their compatibilization efficiency formulated using experimental results for particular systems and/or simplified thermodynamic considerations. It follows from some studies<sup>5–7</sup> that diblock copolymers are more efficient than tri- and multiblocks but other studies arrived at the opposite conclusion.<sup>8–11</sup> Some studies show that copolymers with the block length comparable to the length of the related blend component are the most efficient.<sup>7,12</sup> Other studies concluded<sup>11,13,14</sup> that copolymers with substantially shorter blocks can show a high efficiency. It seems that combination of experimental results with theoretical analysis of the phase structure evolution in polymer blends containing a compatibilizer is necessary for the formulation of reliable rules for the compatibilization efficiency of block copolymers.

Recently, several papers dealing with the description of the phase structure evolution in polymer blends containing a compatibilizer were pub-

Correspondence to: I. Fortelný (forteln@imc.cas.cz).

Contract grant sponsor: Grant Agency of the Czech Republic; contract grant number: 106/02/1248.

Contract grant sponsor: GA AS CR; contract grant number: A4050007.

Contract grant sponsor: The Academy of Sciences of the Czech Republic; contract grant number: AVOZ4050913.

lished.<sup>15–18</sup> These theories are based on the assumption that the distribution of a compatibilizer between the interface and bulk phase is known. A block copolymer would be an ideal compatibilizer if all its chains were localized at the interface until it would be fully covered. In the opposite extreme case, the whole amount of a block copolymer is dissolved or localized as supermolecular objects in a bulk phase. It was found<sup>19</sup> that also in the case when a copolymer is an efficient compatibilizer, it need not behave as an “ideal” compatibilizer, i.e., its whole amount is not localized at the interface.

Kim et al.<sup>20</sup> suggested, using the ratio of the swelling power at the interface of the block copolymer segment outside the droplet to that inside the droplet,  $S_r$ , for prediction of the compatibilization efficiency. Using the results for the poly(cyclohexyl methacrylate)/poly(styrene-*ran*-acrylonitrile) blend compatibilized with poly(styrene-*block*-methyl methacrylate) diblock copolymer, they concluded that block copolymers are inefficient emulsifiers if  $S_r < 0.4$  or  $S_r > 2.5$ . Unstable (coalescence not fully suppressed) and stable emulsifications are predicted for  $1 > S_r > 0.4$  and  $2.5 > S_r > 1$ , respectively. Thermodynamic considerations, which were used in definition of parameter  $S_r$ , are, however, plausible only if the blocks of a copolymer are substantially longer than the chains of the blend components as follows from de Gennes' analysis.<sup>21</sup> Another shortage of the parameter  $S_r$  is that it does not take into consideration the influence of the block copolymer concentration on the interface.

From the commercial point of view, compatibilization of polystyrene/polyolefin blends is very important. These blends are used mostly as packaging materials with balanced mechanical and barrier properties. Moreover, a mixture of a polyolefin with polystyrene is the main part of municipal plastic waste.<sup>22</sup> It was recognized that styrene-butadiene block copolymers, SB, and hydrogenated SB copolymers, SEB, are suitable compatibilizers for these blends.<sup>5,9,13,14,19</sup> SB and SEB copolymers with a broad scale of molecular parameters are produced as thermoplastic elastomers or components of tires. Unfortunately, a criterion for decision, which from available SB and SEB is the most efficient compatibilizer for a certain polystyrene/polyolefin blend, is still lacking.<sup>23</sup> The blocks of commercial SB and SEB copolymers are mostly substantially shorter than the related polystyrene and polyolefin chains. Therefore, the rule formulated by Kim et al.<sup>20</sup> is not applicable.

Leibler<sup>24</sup> evaluated the effect of a block copolymer on interfacial tension between immiscible homopolymers A and B for both long and short copolymer chains. In both the cases, the interfacial tension is reduced if the density of the fixed chains increases. It seems that for a constant interfacial area occupied by

one copolymer chain, long copolymers are more efficient than the short ones.

Formation of micelles in a mixture of homopolymers A, B, and block copolymer A/B was also studied by Leibler.<sup>24</sup> This problem is associated with the density of copolymer molecules on the interface. The derived relations show that critical micellar concentration (cmc) of a block copolymer and its density on the interface depends on the copolymer composition, length of blocks,  $N$ , and interaction parameter,  $\chi_{AB}$ .

Mathur<sup>25</sup> evaluated micellization of asymmetric block copolymers ( $N_A \ll N_B$ ) in a blend of homopolymers of A and B and experimentally proved that the concentration of block copolymer molecules on the interface is controlled by micellization of block copolymer. The surface coverage obtained by Mathur's model calculation for a polystyrene/polybutadiene blend compatibilized with an asymmetric diblock SB copolymer is very low; the surface fraction of the copolymer on the interface is only 0.0013.

It was concluded using the results for polystyrene/polypropylene (PS/PP) blends compatibilized with commercial SB copolymers that in particular the length of styrene blocks in SB copolymers controls their localization in PS/PP blends.<sup>14</sup> For verification of this conclusion, the effect of model diblock (S-B), triblock (S-B-S), and pentablock (S-B-S-B-S) copolymers, with molecular weights of styrene blocks 10,000 or 40,000 and of butadiene blocks 60,000, on the structure and properties of PS blends with PP,<sup>26,27</sup> polybutadiene (PB)<sup>27,28</sup> and high-density polyethylene (HDPE)<sup>29,30</sup> was studied. These studies show that the distribution of SB copolymers between the interface and bulk phases is controlled by the styrene block length rather than by the number of the blocks. In PS/PP and PS/HDPE blends, a part of SB with a short styrene block is localized at the interface. The rest of SB forms particles with the structure of neat SB, which are localized mostly at the interface. Also a part of SB with long styrene blocks is localized at the interface in the studied blends. However, the rest of SB is localized in the PS matrix as small micelles. SB with short styrene blocks showed a larger effect on properties of PS/PP and PS/HDPE blends than the related SB with long styrene blocks.<sup>26,27,30</sup> On the other hand, SB with long styrene blocks showed a higher emulsification ability and improvement of toughness in PS/PB blends.<sup>27,28</sup> In a model PS/PB blend ( $M_{PS} = 40,000$ ,  $M_{PB} = 60,000$ ), an addition of SB with short styrene blocks causes a strong decrease in the size of PB particles during mixing but it does not suppress their strong coalescence during compression molding.<sup>28</sup> It follows from comparison of the effect of SB copolymers with the same length of styrene blocks on the impact strength that triblocks are the most efficient compatibilizers for all the systems under study.

Favis et al.<sup>31</sup> proposed characterization of the compatibilization efficiency by emulsification curves, i.e., the dependence of the size of dispersed particles on the concentration of a compatibilizer relative to the amount of the dispersed phase. They found that the size of dispersed particles decreases with increasing concentration of a compatibilizer until reaches a limit value. The critical concentrations of a compatibilizer,  $c_{cr}$ , at which the limit particle size was achieved, were found between 10 and 20%.<sup>19,26</sup> Li and Favis<sup>19</sup> used comparison of emulsification curves for various concentrations of the dispersed phase for decision if the whole amount of a copolymer is localized at the interface and if at  $c_{cr}$  the copolymer eliminates flow-induced coalescence of dispersed particles. They found that the fraction of *S*-EB-*S* copolymer at the interface decreases with increasing amount of the dispersed phase in a HDPE/PS blend with HDPE matrix and that *S*-EB-*S* does not eliminate flow-induced coalescence of PS particles. The fraction of the *S*-EB-*S* copolymer at the interface in the blends with PS matrix was substantially larger than that with HDPE matrix and the same concentration of the dispersed phase. Li and Favis<sup>19</sup> found that the addition of *S*-EB-*S* triblock leads to a larger decrease in the size of dispersed particles than that of *S*-EB diblock and that *S*-EB-*S* or *S*-EB with long styrene blocks are more efficient than *S*-EB-*S* or *S*-EB with short styrene blocks.

Harrats et al.<sup>23</sup> studied low-density polyethylene/polystyrene (LDPE/PS) (80/20) blends compatibilized with neat *S*-hB and tapered *S*-hBt diblocks with the same molecular weights of styrene and hydrogenated butadiene blocks and with *S*-EB-*S* triblock with long EB and short *S* blocks. The rate of decrease in the size of PS particles with the amount of a copolymer was largest for *S*-hBt and smallest for *S*-EB-*S*. On addition of 10 wt % of a copolymer relative to the blend, i.e., 50 wt % relative to the dispersed phase, more or less the same size of PS particles was achieved for all compatibilizers. The strong decrease in the size of PS particles with increasing concentration of *S*-EB-*S* from 25 wt % to 50 wt % relative to the dispersed phase is surprising. *S*-hB and *S*-hBt stabilized the size of PS particles during annealing but *S*-EB-*S* not.

Mostly it is assumed that a part of a block copolymer, which is not localized at the interface, is dispersed in the bulk phase. Morphology of dispersed copolymer particles is controlled by copolymer composition. The results for the PS/PP and PS/PB blends<sup>14,26,28</sup> discussed above show that SB can exist in these blends as small particles with ordered structure of neat copolymer. Radonjić<sup>13</sup> found that in PP/PS (70/30) blends compatibilized with *S*-B-*S*, PS particles are split by lamellae of *S*-B-*S*. In these blends compatibilized with poly(styrene-*block*-ethylene-*co*-propylene) block copolymer (*S*-EP) or *S*-EB-*S*, agglomerates of PS particles linked with the block copolymer were found.

Fortelný et al.<sup>32</sup> found in a study of high-impact polystyrene (HIPS)/HDPE and HIPS/LDPE blends compatibilized with *S*-B-*S* that the distribution of *S*-B-*S* between the interface and bulk phase is strongly dependent on the blend composition. Also in this study, lamellae of *S*-B-*S* in PS phase (both dispersed and continuous) were detected.

It follows from the above results for polystyrene/polyolefin blends compatibilized with SB, SEB or SEP block copolymers that the structure of these blends strongly depends on the length ratio of blocks and related homopolymer chains and on the interaction parameters,  $\chi$ , between them. Also the number of copolymer blocks plays an important role. It seems that in blends with lower concentrations of the dispersed phase, a larger fraction of the block copolymer is localized at the interface.<sup>19</sup> It has been unclear so far which parameters control the structure of a part of copolymer localized in the bulk phase. It should be mentioned that most theoretical considerations on the compatibilization efficiency have used the rules of equilibrium thermodynamics. However, the structure of polymer blends is generally nonequilibrium. It should be also considered that block copolymers can be above or below the order-disorder transition temperature during mixing of compatibilized blends.<sup>33</sup>

In most papers, the compatibilization efficiency was measured by the compatibilizer effect on the size of dispersed particles and on mechanical properties. Substantially less attention has been paid to the influence of SB copolymers on rheological properties of PS/PE and PS/PP melts.<sup>34</sup> Recently we studied the effect of molecular architecture of SB copolymers on rheological properties of molten PS/HDPE/SB blends.<sup>30</sup> It was found that the effects of the number of blocks in SB copolymers on tensile strength and melt rheological properties of PS/HDPE/SB blends do not correlate.

The aim of this study is to contribute to the elucidation of parameters that determine the distribution of block copolymers between the interface and bulk phase. We shall focus especially on polystyrene/polyolefin blends compatibilized with SB copolymers. Therefore, we shall study dependences of the morphology and impact strength of PS/LDPE blends on the concentrations of model SB copolymers with various numbers of blocks and the length of styrene blocks. For better understanding of the differences between the phase structure of compatibilized blends obtained in melt mixing and that of equilibrium blends, the effect of annealing will be studied. The results of the study will be compared with previous results for compatibilized polystyrene/polyolefin blends. The results will be subjected to thermodynamic analysis of the distribution of a block copolymer between the interface and bulk phase for blends where copolymer blocks have lower molecular weight than the related homopolymers.

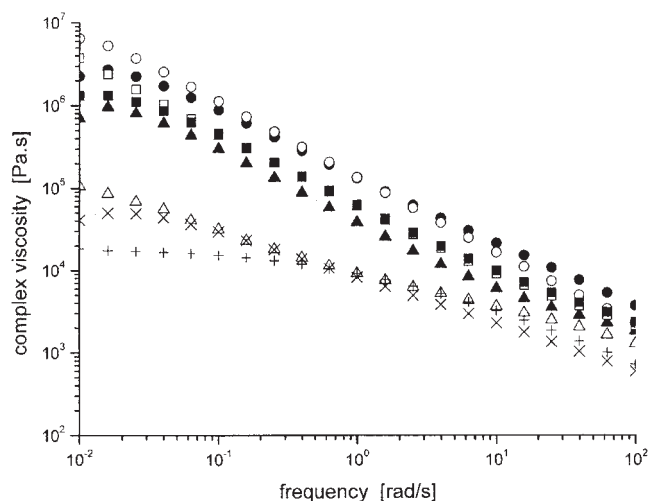


**Figure 1** Dependence of the absolute value of complex viscosity on angular frequency, measured at 190°C, of the used polymers: PS (+), LDPE (×), SB1 (▲), SB2 (■), SB3 (●), SB4 (△), SB5 (□), and SB6 (○).

## EXPERIMENTAL

### Materials

Atactic polystyrene (PS): Krasten 171, commercial product of Kaučuk Co., Kralupy, Czech Republic,  $M_w = 300,000$ ,  $M_w/M_n = 4.6$ .

Low-density polyethylene (LDPE): Bralen RA 2–19, commercial product of Slovnaft a.s., Bratislava, Slovakia, melt flow index MFI (ISO 1133, 190°C, 21.2N) 2 g/10 min, density 918 kg/m<sup>3</sup>,  $M_w = 120,000$ .

Linear styrene–butadiene (SB) block copolymers, a laboratory product of Kaučuk Co., Kralupy, Czech Republic. S-B diblock (SB1), S-B-S triblock (SB2) and S-B-S-B-S pentablock (SB3) with theoretical  $M_w$  of styrene blocks 10,000 and theoretical  $M_w$  of butadiene blocks 60,000; S-B diblock (SB4), S-B-S triblock (SB5), and S-B-S-B-S pentablock (SB6) with theoretical  $M_w$  of styrene blocks 40,000 and theoretical  $M_w$  of butadiene blocks 60,000 were used. All SB samples contain only very small amounts of copolymers with lower numbers of blocks and of styrene homopolymer and they show a very narrow molecular weight distribution. Their detailed molecular characteristics and description of their synthesis can be found in Ref. 28. For all the polymers, the dependence of dynamic viscosity on angular frequency is plotted on Figure 1.

### Blend preparation

Blends with PS/LDPE weight ratio 4/1 containing 0, 2.5, 5, and 10 wt % of SB copolymer (relative to the blend weight) were prepared by mixing the components in the chamber B 50 EHT of a Brabender Plastimeter at the chamber temperature 180°C. The melts were mixed at 120 rpm for 20 min. Quenched samples

for electron microscopy and X-ray scattering were prepared by placing small pieces of the blends into cold water immediately after finishing the mixing. The blend samples used for the determination of the impact strength, X-ray scattering and morphology were shaped from compression-molded plates prepared in a Fontijne press at 190°C and 1.505 MPa for 2 min and 3.1 MPa for another 3 min. After that, the plates were transferred into another press cooled with water. Annealed samples were kept in hot press for 20 min instead of 3 min at 3.1 MPa.

### Scanning electron microscopy of fracture surfaces

Samples were cut from the middle of the prepared polymer blend and fractured in liquid nitrogen. The specimens were fixed at copper supports and coated with platinum to avoid charging. The fracture surfaces were observed in a scanning electron microscope (SEM; microscope Tescan Vega TS 5130), using secondary electrons and accelerating voltage 30 kV.

### Scanning electron microscopy of scratched and etched surfaces

Samples were cut from the middle of the prepared polymer blend, fixed in a basin with liquid nitrogen and scratched with a sharp piece of glass to prepare smooth surface. The specimens with smooth surfaces were removed from liquid nitrogen and etched with a permanganic mixture (0.4 g KMnO<sub>4</sub> in 10 mL H<sub>2</sub>SO<sub>4</sub> and 10 mL H<sub>3</sub>PO<sub>4</sub>). Typical etching times vary around 2 min. The scratched and etched surfaces were examined using the same microscope and the same conditions as in previous paragraph. In this case, LDPE is etched faster than PS and, as a result, the secondary electron micrographs show darker LDPE particles in lighter PS matrix.

### Transmission electron microscopy of OsO<sub>4</sub>-stained ultrathin sections

Small pyramids were cut from the middle of the polymer blends and fixed in an ultramicrotome (Leica Ultracut UCT). The ultrathin sections were transferred onto microscopic grids and stained with OsO<sub>4</sub> vapors. Both scanning electron microscopes equipped with a transmission adapter (STEM; Tescan Vega TS 5130) and transmission electron microscope (TEM; Jeol 200CX) were used to examine the stained ultrathin sections. Under given conditions, the SB compatibilizers, SB<sub>x</sub> ( $x = 1-6$ ), containing double bonds, were stained intensively and PS only slightly. That is why both STEM and TEM micrographs show white PE, light gray PS, and dark gray SB<sub>x</sub>.

### Image analysis

Average particle sizes were determined from SEM micrographs of scratched and etched surfaces. The particle dimensions were measured both manually and automatically (after suitable image processing) using software Lucia (Laboratory Imaging, Czech Republic). The image analysis was complicated by the fact that the particle size distributions were very broad and some particles were irregular in shape. Moreover, there were locations containing predominately smaller particles in many specimens, while in other locations the particles were bigger or more elongated. That is why the image analysis had to be performed with caution, using many particles coming from various locations. The dimensions were characterized in three different ways. All three ways yielded very similar results, i.e., similar phenomenological behavior of the particle size versus the compatibilizer amount, which suggests that the results are reliable.

The first image analysis process was performed as follows: all SEM micrographs available for given sample were carefully examined to find the particle with the smallest diameter (min) and the particle with the highest diameter (max). There were at least three SEM micrographs per each polymer blend. The dimensions of particles were measured with Lucia software using a simple tool for determining distances. Very elongated and irregular particles were excluded from the analysis. The average particle size was then calculated as  $1/2 \times (\text{min} + \text{max})$ . The results are summarized in Figure 4.

In the second image analysis, the dimensions of at least 400 particles for each sample were measured and the average particle size was determined as the arithmetic mean of all the values obtained. The results of the first and second image analyses (cf. Figs. 4 and 5) are in good qualitative agreement, i.e., the absolute values are different, but the trends are similar. The lower values of the average particle size in the second image analysis are due to the smallest particles that dominate the size distributions in all the studied blends and lower the arithmetic means.

The third image analysis was fully automated to avoid human influence. All particles were analyzed, including the elongated and/or irregular particles. The analysis was performed for blends containing the compatibilizer SB3 because these samples contained the most irregular particles. The particles were characterized by their equivalent diameter and mean chord. (Equivalent diameter is defined by  $\text{Eq}_{\text{dia}} = \sqrt{4\text{area}/\pi}$ ). Mean chord is the mean value of secants in directions 0, 45, 90, and 135°. It is suitable not only for characterization of particulate systems but also for characterization of systems with co-continuous phase structure. It is calculated from the area and mean projections according to the formula: mean

chord =  $4\text{area}/(\text{Pr}0 + \text{Pr}45 + \text{Pr}90 + \text{Pr}135)$ ). The results are in accord with those obtained by the second image analysis (cf. Figs. 4 and 5), which confirms that (i) the estimated diameters from the second image analysis are in accord with equivalent diameters and (ii) the estimated diameters from the second image analysis, equivalent diameters and mean chords display the same trends in particle size even though the particles are rather nonisometric.

### Small-angle X-ray scattering (SAXS)

SAXS measurements were performed using an upgraded Kratky camera with a 60- $\mu\text{m}$  entrance slit and 42-cm flight path. Ni-filtered Cu K $\alpha$  radiation (wavelength  $\lambda = 1.54 \text{ \AA}$ ) was used and it was recorded with a position-sensitive detector<sup>35</sup> (Joint Institute for Nuclear Research, Dubna, Russia) for which the spatial resolution is approximately 0.15 mm. The intensities were taken in the range of the scattering vector  $q = (4\pi/\lambda) \sin \theta$  from 0.006 to 0.2  $\text{\AA}^{-1}$  (where  $2\theta$  is the scattering angle). The measured intensities were corrected for sample thickness and transmission, primary beam flux, and sample-detector distance.

### Determination of tensile impact strength

The tensile impact strength,  $a_e$ , was determined at 23°C with a Zwick tester, which was equipped with a special fixture for test specimens according to DIN 53,448. The maximum energy of pendulum was 4 J. Test specimens were cut from press-molded plates. The values of  $a_e$  were determined as arithmetic means of the measurements on 12 specimens.

### Rheological measurements

Flow properties of all blend components and PS/LDPE/SB blends were measured on a rotational rheometer ARES (Rheometric Scientific, Piscataway, NJ) in dynamic mode, using parallel plate and cone-plate geometries (radius 12.5 and 25 mm; cone angle 0.1 rad). The frequency sweep tests were carried out at  $10^{-2}$ – $10^2$  rad/s and 190°C. The experiments were performed in the linear viscoelasticity range and the deformation amplitude was kept small in order not to destroy the microstructure in studied heterogeneous melts.

## RESULTS AND DISCUSSION

The compatibilization efficiency can be estimated from SEM micrographs showing fracture surfaces of PS/LDPE blends (Fig. 2). In the uncompatibilized blends [Figs. 2(a) and 2(b)] the structure is coarse and the LDPE particles are clearly visible as the fracture runs along the interface. This indicates that compatibility of

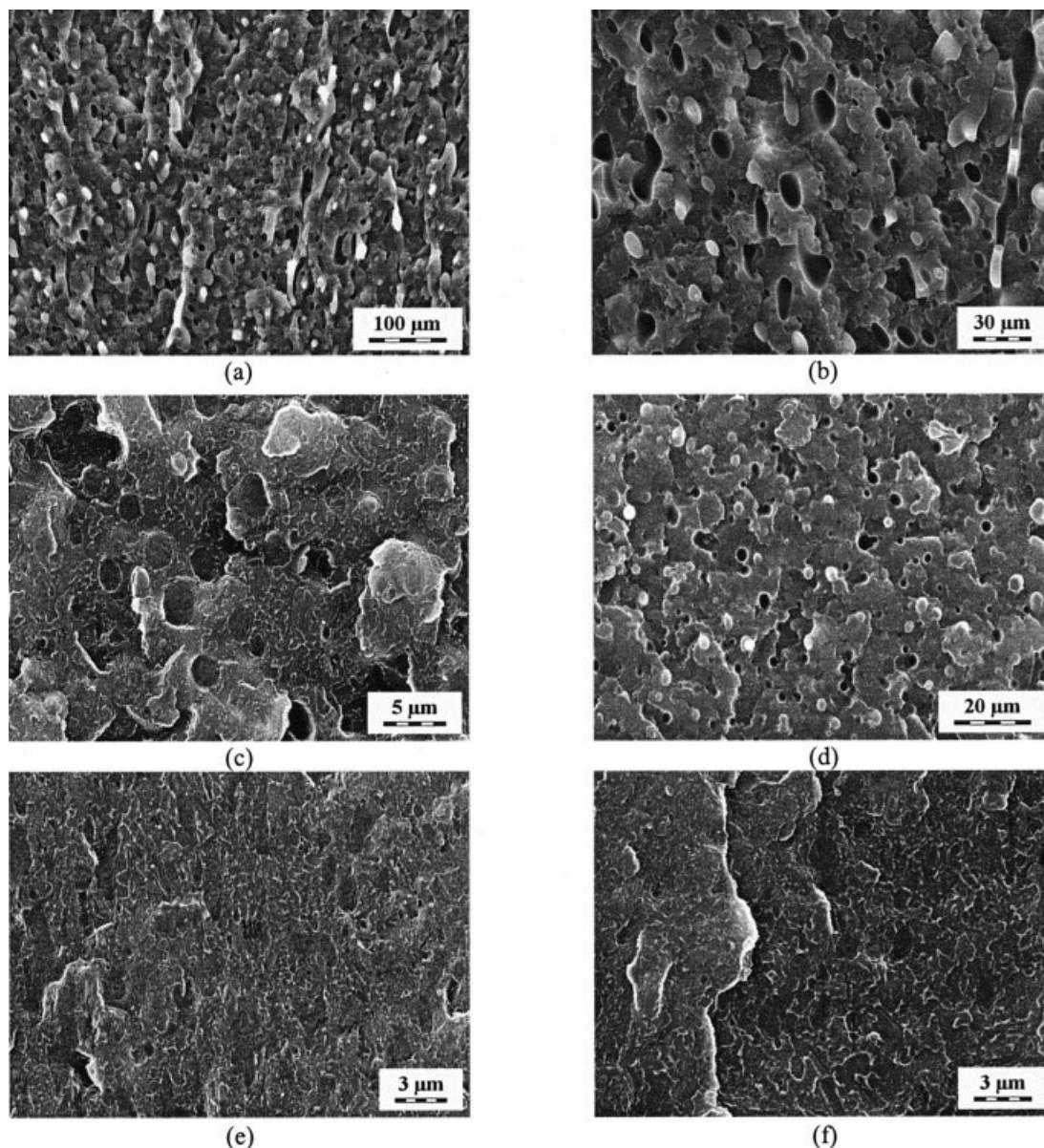


**Figure 2** SEM micrographs of fracture surfaces of PS/LDPE (80/20) blends. Noncompatibilized (a,b), 5% SB2 (c), 5% SB4 (d), 10% SB2 (e), and 10% SB4 (f).

PS and LDPE is rather poor. Addition of 5% of a compatibilizer with short styrene blocks, such as SB2 [Fig. 2(c)], leads to finer structure and fracture running through the particles. The behavior of a blend with 5% of a compatibilizer with long styrene blocks, such as SB4 [Fig. 2(d)], is quite different: the coarseness of the structure slightly decreases but compatibility and interphase adhesion of PS and LDPE is not much improved as the fracture still runs along the interface. Addition of 10% of a compatibilizer to PS/LDPE blends results in fine structure with good compatibility and interphase adhesion of compatibilizers with both short and long styrene blocks [Figs. 2(e) and 2(f)].

In Figure 3, SEM micrographs of compression-molded samples of PS/LDPE blends compatibilized

with 5% of SB copolymers are compared. It can be seen that the size and shape of LDPE particles differ in dependence on SB compatibilizers. The micrographs demonstrate nonuniformity of morphology of the samples described in Experimental Section. The dependences of average particle diameter on the amount of SB copolymers, calculated using the methods described in Experimental Section, are plotted in Figures 4 and 5. In Figure 6, the dependences of the equivalent diameter and mean chord length on the amount of SB3 in the PS/LDPE (80/20) blend are compared. It follows from comparison of Figures 4–6 that average particle sizes determined by various methods somewhat differ. On the other hand, the shapes of the dependences of average particle size on the concen-

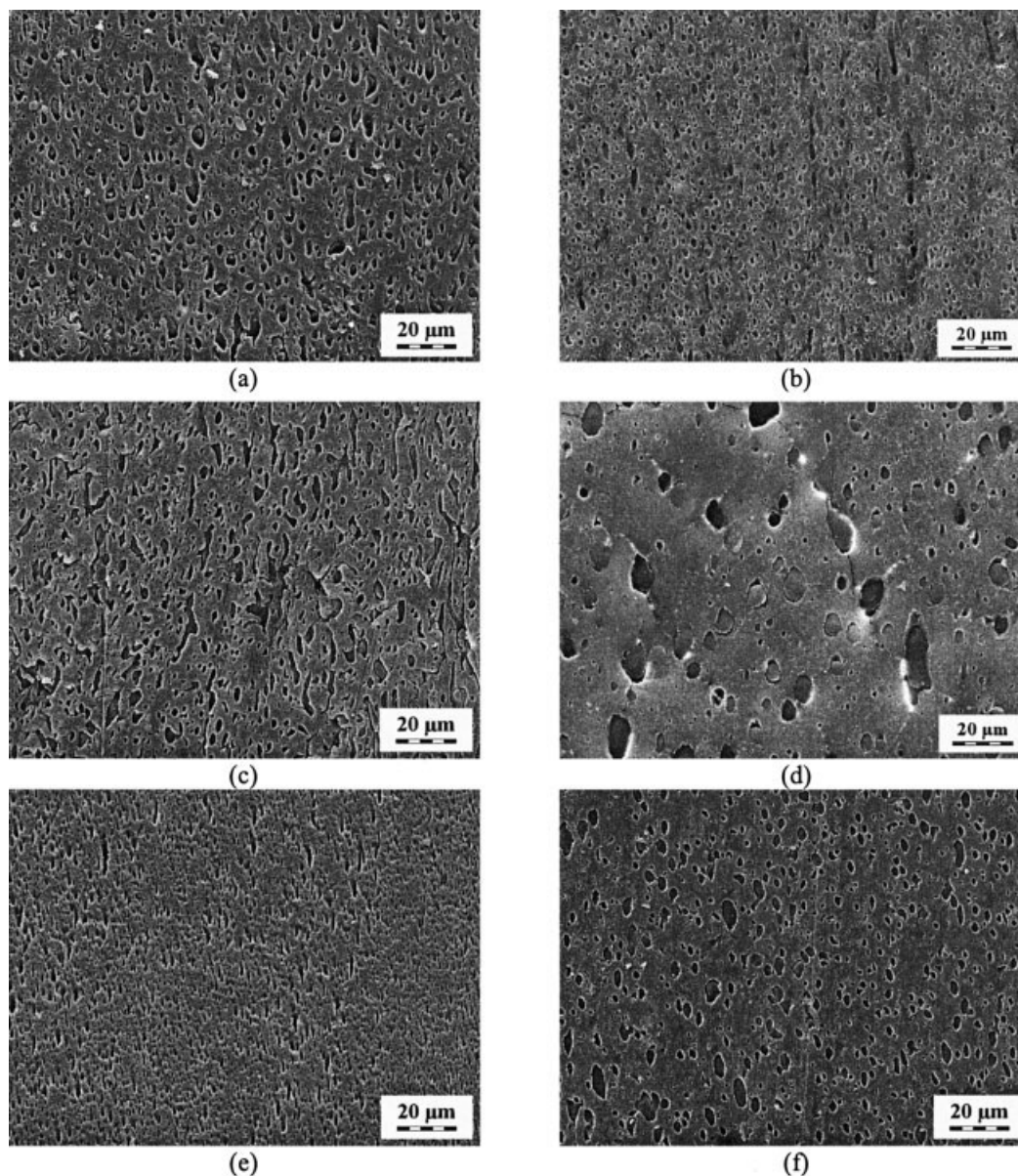


**Figure 3** SEM micrographs of scratched and etched surfaces of PS/LDPE/SB $x$  (80/20/5) blends. SB1 (a), SB2 (b), SB3 (c), SB4 (d), SB5 (e) and SB6 (f).

tration of all SB copolymers are very similar for all methods of particle size determination (cf. Figs. 4–6). A clear difference between the effects of SB copolymers with short (SB1–SB3) and long (SB4–SB6) styrene blocks on the size of LDPE particles follows from Figures 4 and 5. The sizes of LDPE particles in the blends compatibilized with 5 and 10% of SB with short styrene blocks differ only slightly. On the other hand, the increase in the amount of SB copolymer with long styrene blocks from 5 to 10% leads to a pronounced decrease in the size of LDPE particles.

The emulsifying activity of block copolymers A–B in blends of incompatible homopolymers A and B is controlled by molecular parameters of the copolymer. Leibler<sup>24</sup> showed that the spontaneous radius of cur-

vature of an interfacial film is inversely proportional to the copolymer composition asymmetry characterized by the parameter  $\varepsilon = 0.5 - f$ , where  $f$  is composition of the copolymer. The copolymer SB2 is asymmetric with  $f_w = 0.25$  and SB4 is a symmetric copolymer with  $f_w = 0.57$ . Therefore we can expect droplets with smaller radii in blends containing compatibilizer SB2 than in blends compatibilized with SB4.

The decrease in interfacial tension depends on the number of adsorbed copolymer molecules on interface. At a certain concentration of copolymer (saturation limit), we can expect effective interfacial tension  $\gamma$  going to zero ( $\Delta\gamma = \gamma - \gamma_0$ ,  $\Delta\gamma = -\gamma_0$ ).<sup>24</sup> Then we obtain a stable mixture of minority component A in majority matrix B. At that, a problem arises. Asym-

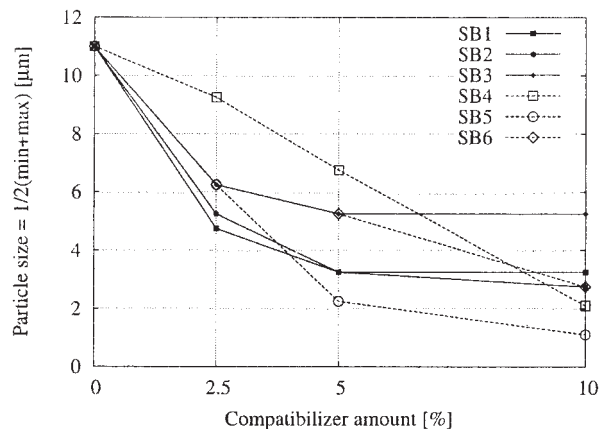


**Figure 4** Average particle diameter in PS/LDPE/SBx blends. The average diameter was calculated as  $\frac{1}{2} \times (\min + \max)$ , where min and max are minimum and maximum of the particle diameter, respectively.

metric block copolymer molecules are able to aggregate and to form micelles above the critical micelle concentration (cmc). Below cmc, the chemical potential of copolymer increases with increasing copolymer concentration and the number of adsorbed copolymer molecules on interface goes up. The interfacial tension decreases.

Above cmc, the concentration of nonaggregated free copolymer molecules remain practically constant and their concentration is given by cmc. The number of adsorbed molecules is also constant and the interfacial tension does not change. The cmc of asymmetric block copolymers is very low.<sup>24,25</sup> The small change of average size of LDPE droplets at concentration 10% of SB2 relatively to 5% concentration shows that cmc was crossed and further addition of the copolymer does not improve emulsification of LDPE.

One of the parameters controlling aggregation of block copolymers is their composition  $f$ . The aggrega-

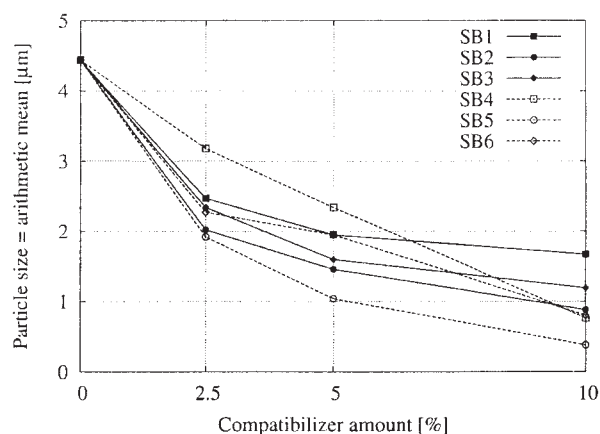


**Figure 5** Average particle diameter in PS/LDPE/SBx blends. The average diameter was determined as the arithmetic mean of diameters for all measured particles.

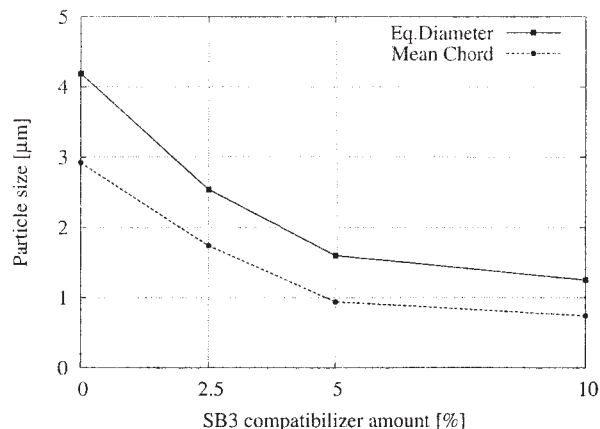


**Figure 6** Particle size in PS/LDPE/SB3 blends. Particle sizes were calculated as equivalent diameter and mean chord.

tion behavior of symmetric and asymmetric block copolymers is therefore a little different. A symmetric copolymer forms lamellae while an asymmetric one forms spherical micelles.<sup>36</sup> Addition of symmetric copolymer increases the number of adsorbed copolymer molecules; there is no restriction given by micellization and the interface can be fully saturated by copolymer molecules. In this case we obtain a stable microemulsion. The estimated concentration of this transition is about 20% of symmetric block copolymer.<sup>37,38</sup> Therefore an increase in SB4 concentration causes a decrease in interfacial tension and the resulting phase structure contain smaller droplets of LDPE.

The dependence of the tensile impact strength,  $a_e$ , of PS/LDPE/SBx blends on the amount of SBx is in full accordance with the related dependence of the LDPE particle size (see Fig. 7). The values of  $a_e$  for blends compatibilized with 5 and 10% of SB with short styrene blocks were practically the same (an increase somewhat exceeding experimental error was observed

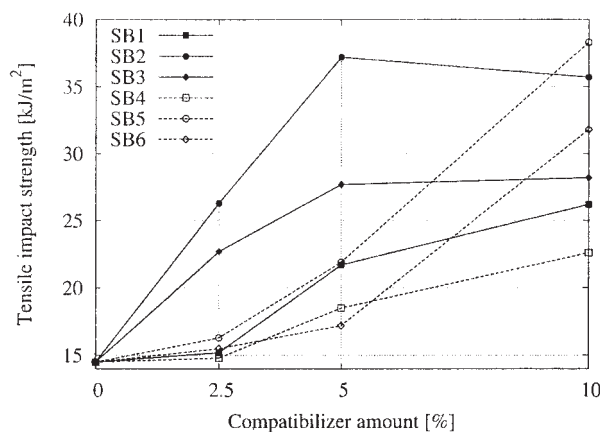


**Figure 7** The dependence of tensile impact strengths in PS/LDPE/SBx blends on concentration of SB copolymers.



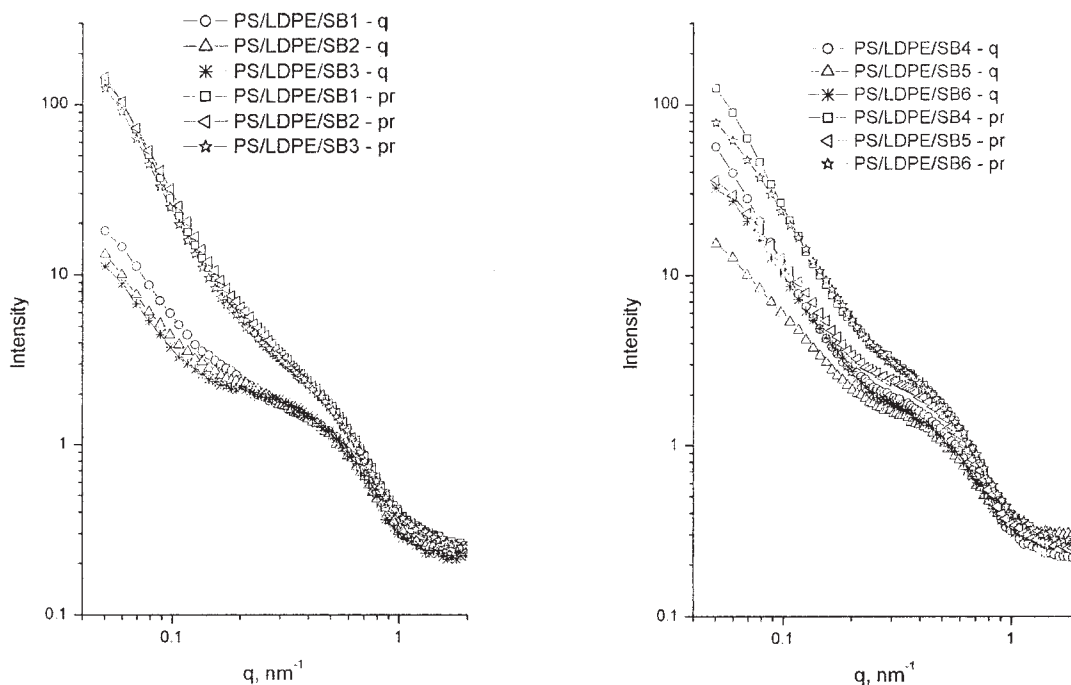


**Figure 8** SAXS curves of PS/LDPE (80/20) + 5% SB $x$ : q, quenched; pr, pressed

only for SB1). A pronounced increase in  $a_e$  was found when the concentration of SB with long styrene blocks (in particular SB5 and SB6) in PS/LDPE/SB $x$  blends increased from 5 to 10%.

SAXS curves of both quenched and slowly cooled samples of PS/PE blends with addition of 5 wt % of each of six block copolymers are shown in Figure 8. On all the curves, a maximum is observed at the scattering vector,  $q = 0.3 \text{ nm}^{-1}$ , corresponding to a long period in semicrystalline LDPE.

In quenched samples with addition of SB1–SB3, i.e., BCs with “short” S blocks (MW of S blocks below the critical value necessary for the entanglement formation),<sup>14,28</sup> other very slight maxima appear, which may correspond to the separated ordered block copolymer phase [Fig. 8]. However, the main feature observed here is a large difference between the SAXS curves of quenched and pressed samples. This suggests significant changes of morphology, proceeding in these samples during cooling.

No additional maxima are observed on SAXS curves of PS/LDPE blends, containing SB4–SB6 copolymers, i.e., those having “long” S blocks, and scattering curves of both quenched and slowly cooled samples are very similar [Fig. 8]. Similar shapes of SAXS curves were found also in PS/PP blends, compatibilized with the same SB copolymers or other block copolymers with “short” and “long” S blocks.<sup>14,26</sup> It was proved that block copolymers having “short” S blocks became a part of the PS/PP interface, remaining the ordered structure of a neat block copolymer, while those with “long” S blocks were entrapped in the PS component

of the PS/PP blends. These block copolymers then lost the ordered structure because of swelling with the S homopolymer.

As large differences in quenched and slowly cooled samples were observed, we prepared also annealed samples (20 min in the hot press, see Experimental section) of PS/LDPE/SB $x$  (75/19/5) blends. In Figure 9, SAXS curves of PS/LDPE blends with addition of 5 wt % SB2 or SB5, prepared under a different temperature regime, are given together with the SAXS curves of corresponding block copolymers. A weak maximum at  $q = 0.24 \text{ nm}^{-1}$  on the SAXS curves of the quenched sample of PS/PE/SB2 suggests the presence of an ordered SB2 phase [Fig. 9]. This maximum nearly vanishes on the scattering curves of the pressed blend. It is possible that SB2 particles, having an ordered structure in the quenched sample, are dispersed here at the PS/LDPE interface but another explanation is also available. As the scattered intensity of the pressed sample strongly increases for  $q < 0.3 \text{ nm}^{-1}$ , probably because of a remarkable change in morphology the formation, which takes place during cooling, the maximum corresponding to the separated SB2 phase is overlapped by this intensity. However, at least a part of SB2 is still regularly organized. As the annealing proceeds, the amount of this ordered phase of SB2 probably increases, as the maximum of the neat SB2 on the SAXS curve of the annealed sample increases. If a blend is formed by two incompatible high homopolymers and a block copolymer, we can observe a large three-phase window consisting of two homopolymer-rich phases and one copolymer-rich

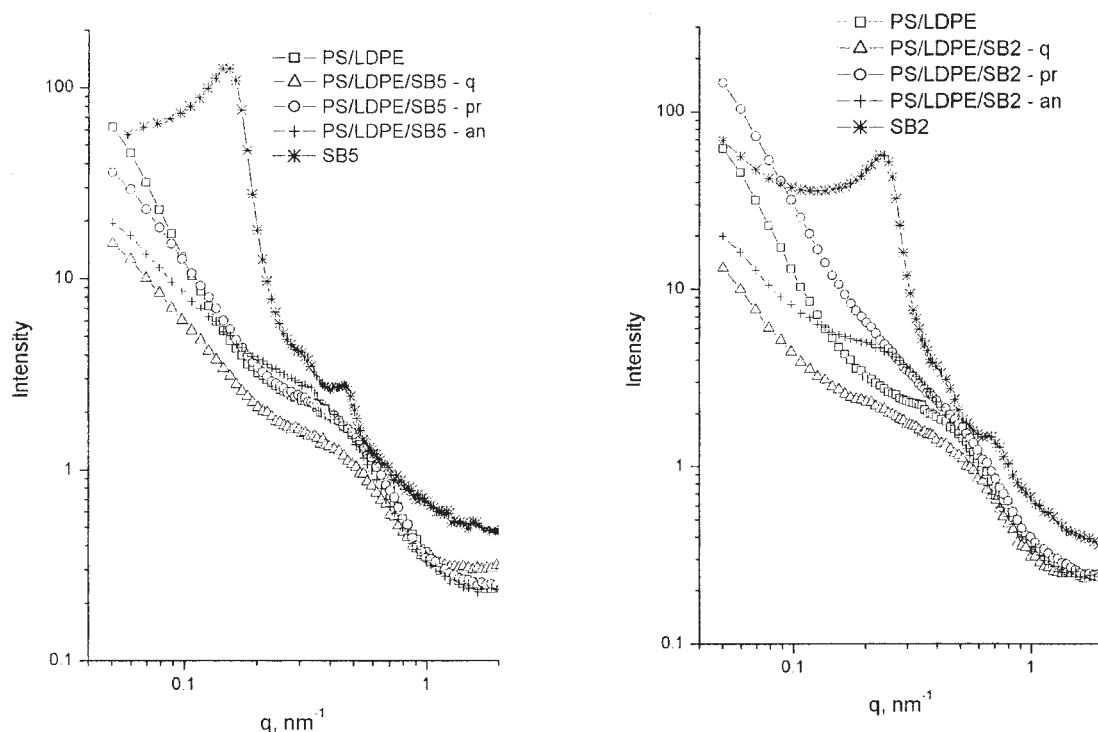


**Figure 9** SAXS curves of PS/LDPE (80/20), PS/LDPE (80/20) +5% SB $x$ , and corresponding SB $x$ : q, quenched; pr, pressed; an, annealed

phase.<sup>39–41</sup> Annealing leads to expulsion of copolymer-rich phase on the interface and, because of low cmc of asymmetric SB2 copolymer, its micelle (organized structure) are formed.

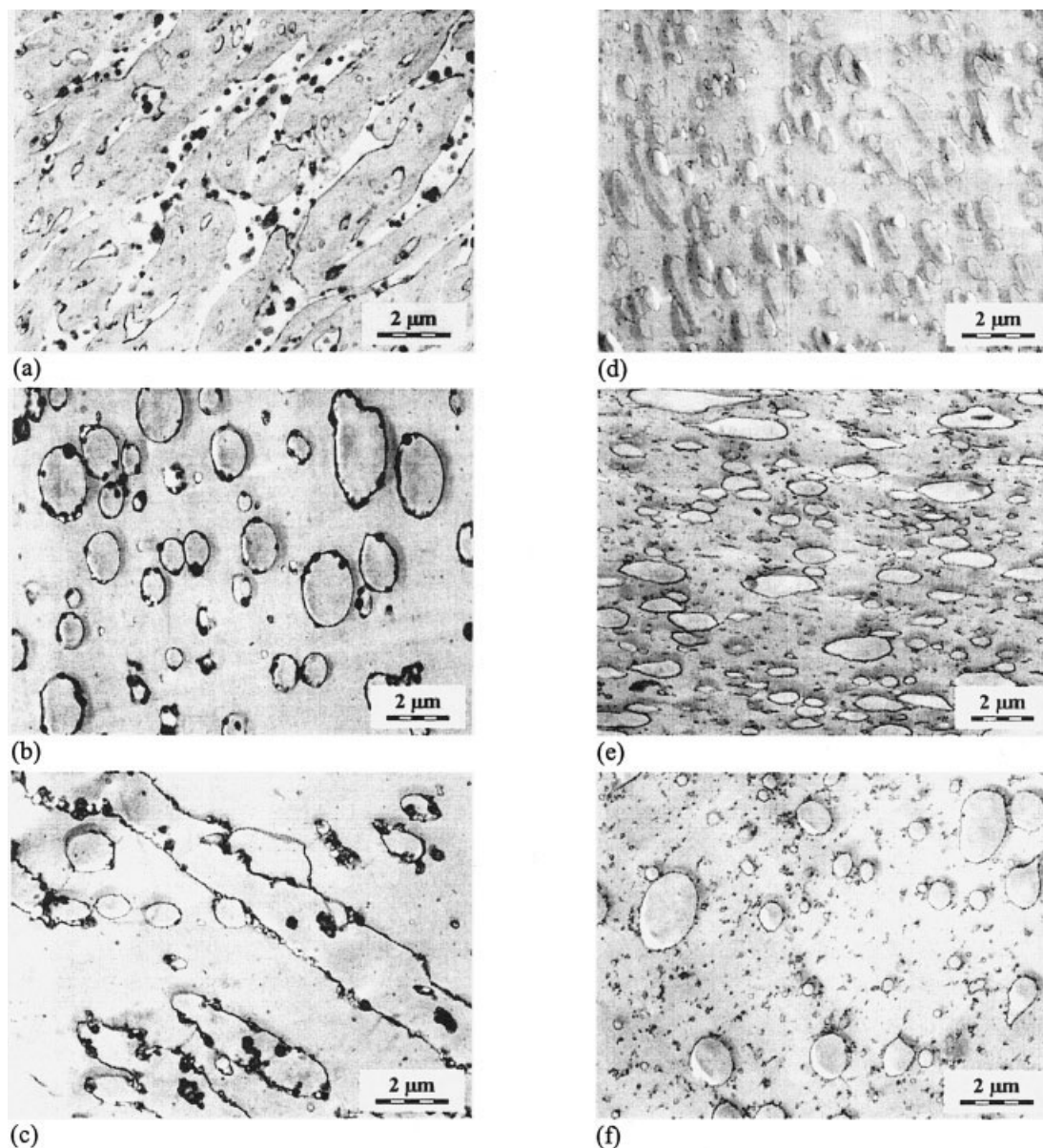
On SAXS curves of all the three types of PS/PE/SB5 blends, quenched, pressed, and annealed, no maxima belonging to the separated ordered SB5 phase are observed [Fig. 9]. So it can be assumed that its structure is lost because of interactions with the PS component of the blend, which can lead to swelling of copolymer particles or to the formation of SB5 micelles.

Figure 10 shows localization of compatibilizers in quenched, pressed, and annealed PS/LDPE/SB2 and PS/LDPE/SB5 blends observed by STEM technique. In quenched PS/LDPE/SB2 blends, the compatibilizer tends to form small particles inside the LDPE phase [Fig. 10(a)], the rest of SB2 forming thin envelopes around LDPE particles. As it was mentioned above, SB2 particles keep the internal structure of the block copolymer. In pressed PS/LDPE/SB2 blends [Fig. 10(b)], the SB2 particles inside the LDPE phase disappear and the compatibilizer is found at the PS/LDPE interface as a thin envelope containing some small SB2 agglomerates. The SB2 agglomerates at the interface do not necessarily lose the internal structure (see above). During further annealing of PS/LDPE/SB2 blends [Fig. 10(c)], the SB2 particles migrate along the interface and coalesce. Reappearing of SB2 particles in the LDPE phase can be tentatively explained as a

consequence of trapping of SB2 particles between coalescing LDPE droplets. The presence of the internal structure of SB2 block polymer is, according to SAXS results, pronounced here.

PS/LDPE/SB5 blend behaves in quite a different way. In quenched blends [Fig. 10(d)], the compatibilizer is mostly localized in the PS matrix and envelopes around the LDPE particles are not developed. This is the result of the nonequilibrium state of quenched blends. During annealing, the particles migrate towards the interface [Fig. 10(e) and 10(f)]. No larger SB5 particles in PS/LDPE/SB5 blends were observed using STEM, which is in agreement with SAXS curves showing no maxima corresponding to larger particles of SB5, which keep the internal structure of the block copolymer [Fig. 9].

The differences in the morphology evolution of PS/LDPE blends compatibilized with a SB copolymer with short or long styrene blocks during annealing manifest themselves also in tensile impact strength. Table I shows that pressed (conventionally) samples of the blends compatibilized with SB copolymers containing short S blocks have higher  $a_e$  than the related annealed blends. The opposite trend was found for the blends compatibilized with SB copolymers containing long S blocks. The observed differences in  $a_e$  match well with differences in coverage of LDPE particles with various SB in the pressed and annealed samples discussed above.



**Figure 10** Localization of compatibilizer in PS/LDPE/SB $x$  (80/20/5) blends. SB2: (a) quenched, (b) pressed, (c) annealed; SB5: (d) quenched, (e) pressed, (f) annealed.

**TABLE I**  
Effect of Annealing on Tensile Impact Strength of PS/  
LDPE/SB $x$  (76/19/5) Blends

Compatibilizer	$a_e$ (kJ/m <sup>2</sup> )	
	Pressed	Annealed
SB1	21.7	19.1
SB2	37.2	29.7
SB3	27.7	26.0
SB4	18.5	23.5
SB5	21.9	27.2
SB6	17.2	25.3

The differences in localization of SB copolymer with short and long S blocks in blends containing 5 and 10% of SB was studied by STEM. The average particle size in PS/LDPE blends with 10% of SB compatibilizers with short-styrene-blocks is not much changed in comparison with the blends with 5% of the same compatibilizer [cf. Figs. 10(b) and 11(a)]. This is in agreement with SEM micrographs [cf. Figs. 2(c) and 2(e)], image analysis [Figs. 4 and 5], and impact strength measurements [Fig. 7]. Addition of larger amounts of the compatibilizer leads to the formation of elongated sheets of the compatibilizer in the matrix; the influence on the average particle size is not so strong. In pressed samples of blends containing 10%

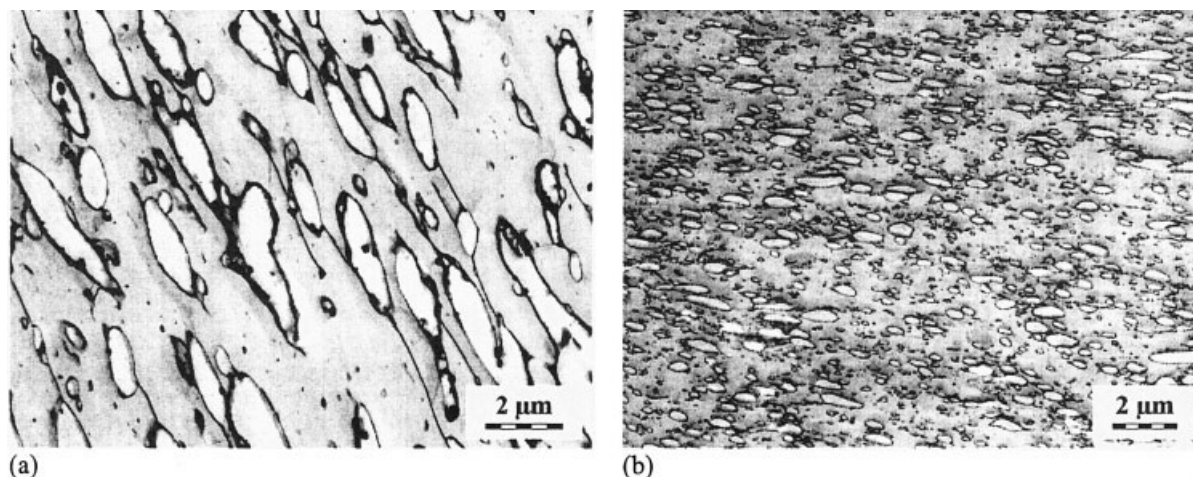


**Figure 11** Localization of compatibilizer in pressed PS/LDPE/SBx (72/18/10) blends. (a) SB2, (b) SB5.

of SB with long styrene blocks, a part of SB forms envelopes of LDPE particles and its rest is dispersed as small particles in the PS matrix similarly to blends containing 5% of the same SB. The average particle size in PS/LDPE blends with 10% of SB containing long styrene blocks decreases significantly in comparison with the blends with 5% of the same compatibilizer [cf. Figs. 10(e) and 11(b)], in accord with the SEM results [cf. Figs. 2(d) and 2(f)], image analysis (Figs. 4 and 5), and tensile impact strength measurements (Fig. 7).

The above results show that the localization of SB copolymers in PS/LDPE (4/1) blends is affected, similarly as in PS/PP and PS/HDPE blends, mostly by the length of styrene blocks, i.e., the asymmetry in block lengths of SB copolymers. The effects of SB1–SB3 copolymers (with short styrene blocks) on the size of LDPE particles and  $a_e$  of PS/LDPE/SBx blends are saturated for 5% of SB. On the other hand, a pronounced decrease in the size of LDPE particles and increase in  $a_e$  of PS/LDPE/SBx blends were found if the content of SB4–SB6 increased from 5 to 10%. This difference between the effects of SB with short and long styrene blocks can be explained as a consequence of the above discussed low cmc of asymmetric block copolymers and different behavior of symmetric and asymmetric copolymers. The amount of the symmetric copolymer at the interface is not controlled by cmc but by equilibrium with SB lamellae swollen with PS. However, it should be mentioned that besides geometrical asymmetry, the  $\chi$  parameters of blocks with the related blend components are not symmetric— $\chi$  between PB and LDPE is low but positive. All these considerations are applicable also to PS/HDPE and PS/PP blends and to polystyrene/polyolefin blends compatibilized with SEB block copolymers.

Dependences of  $\eta^*$  (see Fig. 1) and storage modulus (not reproduced here) on frequency for all SB

copolymers except SB4 show that these copolymers are below the order–disorder transition temperature,  $T_{ODT}$ , at mixing temperature ( $\sim 190^\circ\text{C}$  in melt). In spite of this fact, the copolymers show a compatibilization effect and a qualitative difference in compatibilization efficiency of SB4, which seems to have a different ordered structure than other SB copolymers according to  $\eta^*$  (SB4 shows a strong birefringence at  $190^\circ\text{C}$  and, therefore, is not above  $T_{ODT}$ ),<sup>42</sup> and other SB copolymers was not detected. Moreover, SB5 and SB6 fully lost their ordered structure in PS/LDPE blends and pronounced migration of SB5 at the interface during annealing below  $T_{ODT}$  was detected. These results show that the fact that block copolymers are below  $T_{ODT}$  does not exclude their use as compatibilizers. On the other hand, the above results do not exclude that the relation between mixing temperature and  $T_{ODT}$  of a compatibilizer affects its compatibilization efficiency.<sup>33</sup>

The migration of SB copolymers between the interface and bulk phases during annealing of PS/LDPE/SB blends, described above, clearly shows that the localizations of compatibilizers in blends under steady mixing and at equilibrium are generally not the same. To the same conclusion lead also Maric's and Macosko's results,<sup>43</sup> who found that symmetric block copolymers with substantially shorter block lengths than those of blend components show a strong emulsification effect at mixing but they poorly stabilize the system against coalescence during annealing. Therefore, the rules derived for localization of a compatibilizer in polymer blends based on considerations of equilibrium thermodynamics have only a limited applicability to polymer blends prepared by melt mixing. On the other hand, the above results show that mechanical properties of compatibilized polymer blends in some cases can be substantially improved by optimizing their processing conditions.

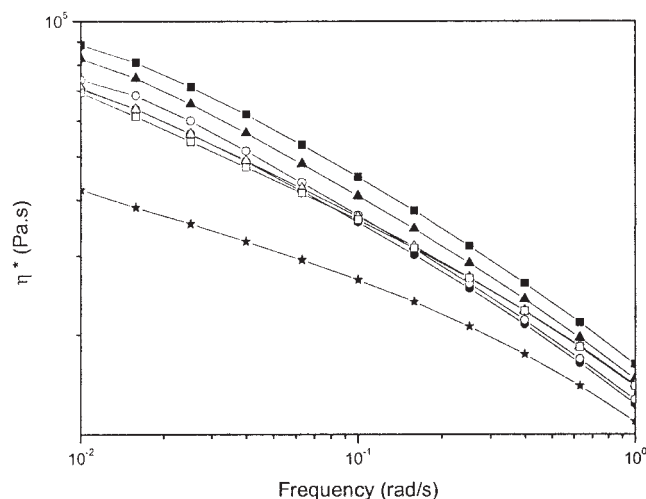


**Figure 12** Dependence of the absolute value of complex viscosity,  $\eta^*$  of the PS/LDPE/SB $x$  blends on angular frequency measured at 190°C.; uncompatibilized (★), SB1 (●), SB2 (▲), SB3 (■), SB4 (○), SB5 (△), and SB6 (□).

All PS/LDPE/SB $x$  (76/19/5) blends have substantially higher complex viscosity than the PS/LDPE (80/20) blend (see Fig. 12). The difference between  $\eta^*$  for PS/LDPE blend without a compatibilizer and blends compatibilized with 5% of SB having long styrene blocks (SB4–SB6) is substantially higher than for related blends with HDPE (cf. Fig. 12 with Fig. 3 in Ref. 30<sup>30</sup>). At low angular frequencies,  $\eta^*$  decreases in the order PS/LDPE/SB4 > PS/LDPE/SB5 > PS/LDPE/SB6. At  $\omega > 10^{-1}$  rad/s,  $\eta^*$  for PS/LDPE/SB5 and PS/LDPE/SB6 is practically the same and higher than that for the PS/LDPE/SB4 blend. The blends compatibilized with SB having short styrene blocks (SB1–SB3) show a stronger dependence on the number of blocks than do the blends with SB having long styrene blocks. In the whole frequency range,  $\eta^*$  increases in the order PS/LDPE/SB1 < PS/LDPE/SB2 < PS/LDPE/SB3, i.e., with increasing number of blocks in SB copolymers. This is qualitatively different from compatibilized PS/HDPE blends, where the blend compatibilized with SB1 shows a higher viscosity than the blends compatibilized with SB2 and SB3. Dependences of  $\eta^*$  for PS/LDPE/SB $x$  blends on the number of blocks in SB $x$  do not correlate with the related dependences of the tensile impact strength for SB with either short or long styrene blocks, which show maximum for triblocks.

The effect of SB copolymers on rheological properties of PS/LDPE/SB blends is not easy to interpret. Generally, the compatibilizer induces an increase in the blend viscosity due to a decreased slip at the interface. The second contribution of a compatibilizer comes from copolymer molecules and/or particles dispersed in bulk phases, especially in the matrix. The first effect of a compatibilizer on the viscosity should

correlate with its effect on the impact strength—depression of the interfacial slip should correlate with a decrease in the size of minor phase particles and adhesion at the interface. On the other hand, the other contribution of a compatibilizer to the blend viscosity need not correlate with the impact strength. Unfortunately, we have not enough information about the nature of SB particles in the systems under study for reliable estimation of this contribution.

The above and literature experimental results and thermodynamic considerations for polystyrene/polyolefin blends compatibilized with SB block copolymers show that the compatibilization efficiency of the copolymers (assessed by fineness of the phase structure and mechanical properties of the blends) depends not only on their molecular architecture but also on the polystyrene/polyolefin ratio in a blend,<sup>19,32,44</sup> on the concentration of a copolymer<sup>23</sup> and on the mixing and processing conditions.<sup>29,44</sup> Therefore, it is impossible to formulate a general rule for selection of an optimum SB copolymer for a certain polystyrene/polyolefin pair, which was the aim of many previous studies.<sup>5–14,26,27,30,33</sup>

As it was mentioned in the discussion of SEM micrographs, nonuniform distribution of LDPE particles (rather large domains with smaller and bigger particles) in PS/LDPE blends with and without a compatibilizer was found. Several years ago, this type of morphology was found in PS/PP blends.<sup>45–48</sup> The nonuniformity persisted on long and intensive mixing and it was not substantially suppressed by the addition of a compatibilizer. It was substantially suppressed only by an increase in mixing temperature. The origin of this type of nonuniformity of the phase structure is not clear.<sup>47,48</sup>

## CONCLUSIONS

Image analysis of PS/LDPE/SB $x$  blends was complicated by broad particle size distribution, irregular shapes of the particles and variable particle size depending on location. Despite these facts, careful image analysis, performed in three different ways, yielded reasonable and reproducible results. The precision of the results might be limited, but the differences in the particle sizes in the blends, caused by various compatibilizers, are clearly visible.

The localization of SB copolymers with a short (SB1–SB3) and long (SB4–SB6) styrene blocks in PS/LDPE/SB $x$  blends was qualitatively different and similar to the same copolymers in PS/HDPE/SB and PS/PP/SB blends. The effect of SB1–SB3 copolymers on the size of LDPE particles and on the tensile impact strength,  $a_e$ , was saturated at 5% (relative to whole blends) of SB copolymers. A pronounced decrease in the LDPE particle size and an increase in  $a_e$  were found when the concentration of SB4–SB6 increased from 5 to 10%.

From thermodynamic analysis it follows that the main reason for different behavior of PS/LDPE blends compatibilized with SB1–SB3 or SB4–SB6 copolymers is the difference in composition asymmetry of the copolymers.

Pronounced changes in the localization of SB copolymers during annealing of PS/LDPE/SB<sub>x</sub> blends were detected. SB1–SB3 particles moved from the LDPE phase at the interface where coalesced and this was followed by a decrease in  $a_e$  of PS/LDPE/SB blends. On the other hand, SB4–SB6 copolymers moved during annealing from the PS phase at the interface, which was followed by an increase in the  $a_e$  of the blends. Substantial migration of SB copolymers during annealing shows that their distribution between the interface and bulk phases in steady state (during mixing) and at thermodynamic equilibrium is not the same.

The effect of molecular structure of SB copolymers on viscosity of PS/LDPE/SB<sub>x</sub> blends does not correlate with its effect on the tensile impact strength of these blends and it qualitatively differs from this effect on viscosity of PS/HDPE/SB<sub>x</sub> blends.

The compatibilization efficiency of SB and SEB block copolymers with blocks shorter than the compatibilized polymers for a certain polystyrene/polyolefin pair is not a function of the copolymer molecular structure only. It depends also on the ratio of blend components, copolymer concentration in a blend, and mixing and processing conditions.

## References

- Bonner, J. G.; Hope, P. S. In *Polymer Blends and Alloys*; Folkes, M. J., Hope, P. S., Eds.; Blackie Academic and Professional: London, 1993.
- Hermes, H. E.; Higgins, J. S. *Polym Eng Sci* 1998, 38, 8477.
- Di Lorenzo, M. L.; Frigione, M. *J Polym Eng* 1997, 17, 429.
- Anastasiadis, S. H.; Gancarz, I.; Koberstein, J. T. *Macromolecules* 1989, 22, 1449.
- Fayt, R.; Jérôme, R.; Teysié, P. *J Polym Sci Part B: Polym Phys* 1989, 29, 945.
- Taha, M.; Frerejean, V. *J Appl Polym Sci* 1996, 61, 969.
- Xu, G.; Lim S. *Polymer* 1996, 37, 421.
- Kroeze, E.; ten Brinke, G.; Hadziioannou, G. *Polym Bull* 1997, 38, 203.
- Horák, Z.; Fořt, V.; Hlavatá, D.; Lednický, F.; Večerka, F. *Polymer* 1996, 37, 65.
- Haage, S.; Friedrich, C. *Polym Networks Blends* 1994, 4, 61.
- Appleby, T.; Czer, F.; Moad, G.; Riiyardo, E.; Stavropoulos, C. *Polym Bull* 1994, 32, 479.
- DelGuidice, L.; Cohen, R. E.; Attalla, G.; Bertinotti, F. J. *J Appl Polym Sci* 1985, 30, 4305.
- Radonjič, G.; Musil, V.; Šmit, I. *J Appl Polym Sci* 1999, 72, 291.
- Hlavatá, D.; Horák, Z.; Hromádková, J.; Lednický, F.; Pleska, A. *J Polym Sci Part B: Polym Phys* 1999, 37, 1647.
- Tang, T.; Huang, B. *Polymer* 1994, 35, 281.
- Milner, S. T.; Xi, H. *J Rheol* 1996, 40, 663.
- Fortelný, I.; Živný, A. *Polymer* 2000, 41, 6865.
- Van Puyvelde, P.; Velankar S.; Moldenaers, P. *Curr Opin Colloid Interface Sci* 2001, 6, 457.
- Li, J.; Favis, B. D. *Polymer* 2002, 43, 4935.
- Kim, J. R.; Jamieson, A. M.; Hudson, S. D.; Manas-Zloczower, I.; Ishida, H. *Macromolecules* 1999, 32, 4582.
- de Gennes, P. G. *Macromolecules* 1980, 13, 1069.
- Fortelný, I.; Kruliš, Z.; Michálková, D. *Polimery (Warsaw)* 2002, 47, 534.
- Harrats, C.; Fayt, R.; Jérôme, R. *Polymer* 2002, 43, 863.
- Leibler, L. *Makromol Chem Macromol Symp* 1988, 16, 1.
- Mathur, D.; Hariharan, R.; Nauman, E.B. *Polymer* 1999, 40, 6077.
- Hlavatá, D.; Horák, Z.; Lednický, F.; Hromádková, J.; Pleska, A.; Zanevski, Yu. V. *J Polym Sci Part B: Polym Phys* 2001, 39, 931.
- Horák, Z.; Hlavatá, D.; Fortelný, I.; Lednický, F. *Polym Eng Sci* 2002, 42, 2042.
- Horák, Z.; Hlavatá, D.; Hromádková, J.; Kotek, J.; Hašová, V.; Mikešová, J.; Pleska, A. *J Polym Sci Part B: Polym Phys* 2002, 40, 2612.
- Fortelný, I.; Hlavatá, D.; Mikešová, J.; Michálková, D.; Potroková, L.; Šloufová, I. *J Polym Sci Part B: Polym Phys* 2003, 41, 609.
- Fortelný, I.; Mikešová, J.; Hromádková, J.; Hašová, V.; Horák, Z. *J Appl Polym Sci* 2003, 90, 2303.
- Favis, B. D.; Cigana, P.; Matos, M.; Tremblay, A. *Can J Chem Eng* 1997, 75, 273.
- Fortelný, I.; Michálková, D.; Hromádková, J.; Lednický, F. *J Appl Polym Sci* 2001, 81, 570.
- Chun, S. B.; Han, C. D. *Macromolecules* 1999, 32, 4030.
- Brahimi, B.; Ait-Kadi, A.; Aiji, A.; Jerome, R.; Fayt, R. *J Rheol* 1991, 35, 1069.
- Chernenko, S. P.; Cheremukhina, G. A.; Fateev, O. V.; Smykov, L. P.; Vasiliev, S. E.; Zanevsky, Y. V.; Kheiker, D. M.; Popov, A. N. *Nucl Instrum Methods Phys Res* 1994, A348, 261.
- Leibler, L. *Macromolecules* 1980, 13, 1602.
- Messé, L.; Corvazier, L.; Ryan, A. J. *Polymer* 2003, 44, 7397.
- Thompson, R. B.; Matsen, M. W. *J Chem Phys* 2000, 112, 6863.
- Leibler, L. *Makromol Chem Rapid Commun* 1981, 2, 393.
- Broseta, D.; Fredrickson, G. H. *J Chem Phys* 1990, 93, 2927.
- Lee, J.; Ruegg, M. L.; Balsara, N. P.; Zhu, Y.; Gido, S.; Krishnamoorti, R.; Kim, M. -H. *Macromolecules* 2003, 36, 6537.
- Štěpánek, P.; Černoch, P. unpublished results.
- Maric, M.; Macosko, C. W. *J Polym Sci Part B: Polym Phys* 2002, 40, 346.
- Hlavatá, D.; Hromádková, J.; Fortelný, I.; Hašová, V.; Pulda, J. *J Appl Polym Sci* 2004, 92, 2431.
- Fortelný, I.; Michálková, D.; Mikešová, J. *J Appl Polym Sci* 1996, 59, 155.
- Navrátilová, E.; Fortelný, I. *Polym Networks Blends* 1996, 6, 127.
- Fortelný, I.; Michálková, D. *Polym Networks Blends* 1997, 7, 125.
- Fortelný, I.; Michálková, D. *Plast Rubber Compos Process Appl* 1998, 27, 53.